Hu Wang
The State Key Laboratory of Advanced Technology for Vehicle Design and Manufacture, College of Mechanical and Vehicle Engineering, Hunan University, Changsha, Hunan, P. R. China
e-mail: wanghuenying@hotmail.com

Songqing Shan
Department of Mechanical and Manufacturing Engineering, University of Manitoba, Winnipeg, MB, R3T 5V6, Canada
e-mail: shans@cc.umanitoba.ca

G. Gary Wang
School of Engineering Science, Simon Fraser University, Surrey, BC, V3T 0A3, Canada
e-mail: gary_wang@sfu.ca

Guangyao Li
The State Key Laboratory of Advanced Technology for Vehicle Design and Manufacture, College of Mechanical and Vehicle Engineering, Hunan University, Changsha, Hunan, P. R. China
e-mail: gyli@hnu.cn

Integrating Least Square Support Vector Regression and Mode Pursuing Sampling Optimization for Crashworthiness Design

Many metamodeling techniques have been developed in the past two decades to reduce the computational cost of design evaluation. With the increasing scale and complexity of engineering problems, popular metamodeling techniques including artificial neural network (ANN), Polynomial regression (PR), Kriging (KG), radial basis functions (RBF), and multivariate adaptive regression splines (MARS) face difficulties in solving highly nonlinear problems, such as the crashworthiness design. Therefore, in this work, we integrate the least support vector regression (LSSVR) with the mode pursuing sampling (MPS) optimization method and applied the integrated approach for crashworthiness design. The MPS is used for generating new samples which are concentrated near the current local minima at each iteration and yet still statistically cover the entire design space. The LSSVR is used for establishing a more robust metamodel from noisy data. Therefore, the proposed method integrates the advantages of both the LSSVR and MPS to more efficiently achieve reasonably accurate results. In order to verify the proposed method, well-known highly nonlinear functions are used for testing. Finally, the proposed method is applied to three typical crashworthiness optimization cases. The results demonstrate the potential capability of this method in the crashworthiness design of vehicles. [DOI: 10.1115/1.4003840]

1 Introduction

Vehicle crashworthiness is of great importance today to the automotive industry. A good rating in crashworthiness gives an automaker a strong argument for sales. Therefore automakers strive to improve the vehicle crashworthiness through design optimization. The crashworthiness optimization, however, normally requires a large number of crash simulations to achieve the optimal design. With the increasing complexity and scale of finite element analysis (FEA) crashworthiness model, the computational cost becomes extremely high and even unacceptable for engineering practice. Therefore, metamodeling techniques are often applied in the crashworthiness design. In the past two decades, various metamodeling techniques have been applied in crashworthiness optimization, including polynomial regression response surface methodology (PR-RSM) [1–6], successive RSM [1], KG [3,4,7], moving least square method (MLS) [3], RBF [3,6], adaptive and interactive modeling system (AIMS) [3], space mapping (SM)-based metamodeling [8], and so on.

Some authors also compared the performance of different metamodel-based optimization algorithms. Comparisons for crashworthiness problems can be found in the studies of Gu [2], Yang et al. [3], Forsberg et al. [5], and Fang et al. [6]. These works tried to determine which metamodel technique(s) might be preferable for crashworthiness design and what are the relative benefits and drawbacks of these methods in an iterative optimization procedure. Gu [2] described the current state-of-the-art of the approximation methods used by Ford Motor Company. Based on the study on stepwise regression (SR), MLS, KG, multiquadric (MQ), and AIMS, Yang et al. [3] pointed out that for a small sample size $<9n$ (where n denotes the number of design variables), no method consistently outperforms the other methods in terms of the accuracy and convergence rate. A simpler and less computational intensive method may be preferable, e.g., quadratic response surface model. For a larger sample size $>9n$, all methods appear to perform much more consistently; complex metamodels such as KG, MLS, and MQ tend to outperform SR. The focus of Forsberg et al. [5] was to compare the performance between KG and PR-RSM. Forsberg et al. [5] concluded that KG was more promising than PR-RSM, but PR-RSM seemed to be able to find a feasible design point more easily. According to the conclusion of Fang et al. [6], RBF was found to generate better models than PR-RSM, based on the same number of the sample points, but PR-RSM was more stable. After all, these researches do not provide a definitive conclusion on which metamodel is the best. Generally we learned that the interpolation methods, such as KG and RBF, might construct more accurate but less stable models as compared with PR-RSM. How to choose the "right" metamodel technique for crashworthiness problems, however, remains an open issue.

In our opinions, the challenges of crashworthiness optimization for metamodel-based approaches mostly arise from the following two avenues.

I. The crashworthiness optimization relies heavily on the accuracy and stability of the vehicle FEA model. Due to the high nonlinearity of the problem, as well as imperfection of numerical methods and uncertainties in simulation, such as hourglass, buckling, and material parameters, the simulation might not completely match the physical experiment results. Furthermore, the FEA solver, such as the parallel explicit FEA simulation code, might not even obtain the same response with the same input parameters. In other words, noisy points might be present in the design space. Therefore, interpolation-based metamodels, such as the commonly used KG and RBF which pass through the sample points, are

Contributed by the Design Automation Committee of ASME for publication in the JOURNAL OF MECHANICAL DESIGN. Manuscript received September 22, 2009; final manuscript received February 24, 2011; published online May 9, 2011. Assoc. Editor: Timothy W. Simpson.

inadequate in filtering the noisy points. Although KG could be modified to accommodate noises, the modeling process requires calling of a global optimization routine, which makes the modeling complex and unreliable. On the other hand, although the polynomial regression (PR)-based metamodel can construct smooth models, the accuracy of response surface models is usually too poor to be acceptable in practice.

II. The crash simulation requires extensive computational resource and time. Therefore, the crashworthiness optimization should be performed with as a few simulation evaluations as possible. Most of the current metamodeling techniques could not deliver the desired accuracy to be useful in practice with only a very limited number of simulations. As a result, the critical issue is how to obtain the optimum effectively with little resource.

The purpose of this study is to integrate appropriate sampling and metamodeling strategies to develop an alternative crashworthiness optimization approach. Such an approach should satisfy at least two basic conditions for the crashworthiness optimization as follows

I. The approach is sufficiently robust to avoid distractions from the noises and outlier points;
II. The approach is efficient to converge in acceptable time.

For the first requirement, support vector regression (SVR) is employed to build metamodels in this study. Most frequently used metamodeling techniques are based on empirical risk minimization (ERM). The major bottleneck of these techniques is the lack of generalization ability and robustness. Compared with the ERM-based metamodeling techniques, SVR is based on structure risk minimization (SRM). Unlike traditional methods which minimize the empirical training error, SVR aims to minimize the upper bound of the generalization error through maximizing the margin between the separating hyperplane and data. In the past few years, several studies [9–12] have successfully applied SVR to function estimation. According to Ref. [13], the SVR-based metamodeling technique achieves more accurate and more robust function approximations than RSM, KG, RBF, and MARS. It also demonstrated that SVR was an alternative technique for approximating complex engineering analyses. Recently, a least square (LS) version of the SVR (LSSVR) technique has received attention for function estimation [14]. In LSSVR, Vapnik's ε-insensitive loss function has been replaced by a sum-squared error cost function. According to the theory of LSSVR, LSSVR is reformulation to the standard SVRs which leads to solving a linear Karush-Kuhn-Tucker (KKT) system. This reformulation greatly simplifies a problem such that the LSSVR solution follows directly from solving a set of linear equations [14].

The second challenge that needs to be addressed is the efficiency of metamodeling and optimization procedure. An active branch of research in metamodeling is on adaptive sampling strategy that can improve the accuracy of metamodels. As early as in the 1960s, Box and Draper [15] suggested a method to refine the response surface (RS) to capture the actual function by screening out unimportant variables. Chen et al. [16] suggested heuristics to lead the surface refinement to a smaller design space. Wujek and Renaud [17,18] compared several move-limit strategies that focus on controlling the function approximation in a more meaningful design space. Toropov et al. [19] suggested the use of a sequential metamodeling approach using move limits. Alexandrov et al. [20] incorporated a trust region method with metamodeling technique. Jones et al. [21] developed an efficient global optimization (EGO) approach based on the KG and adaptive sampling on areas leading to more "expected improvement" of the model accuracy. Wang and Simpson [22] developed a fuzzy clustering based hierarchical metamodeling for design space reduction and optimization. Wang and Li proposed a particle swarm optimization intelligent sampling (PSOIS) [7] and boundary and best neighbor sampling (BBNS) [23] for enhancing the accuracy and efficiency of metamodels, respectively, and developed parallel BBNS [24] for sheet forming successfully. Wang et al. [25] developed an MPS method, which has been successfully applied to solving many benchmarks as well as engineering design problems with continuous variables and, later on, mixed variables [26].

MPS uses a sampling guidance function established based on the initial sample points to determine the sampling path, and the evaluations are based on a metamodel. The advantage of the space reduction strategies is that newly generated samples are concentrated near the current local minima of the design space and yet still statistically cover the entire design space. The drawback of the MPS [25] is that a simple RBF model is employed to establish the sampling guidance function; the accuracy and reliability of the RBF-based metamodel determine the sampling direction and focus. As mentioned before, it makes the MPS inapplicable for problems with noises and outlier points due to the interpolation characteristics of the RBF. To conquer this bottleneck, the LSSVR is introduced to construct metamodels in the proposed approach. Furthermore, to achieve more accurate metamodel efficiently, the MPS is also modified in this study.

The rest of this paper is organized as follows. Section 2 describes the fundamentals of the MPS and LSSVR. The assessment of performance of the proposed method is described in Sec. 3. In Sec. 4, the proposed method is applied to crashworthiness design. Conclusions are given in Sec. 5.

2 Related Theories

In this section, the basic theories of the LSSVR are briefly introduced [14]. According to the comparison tests by Clarke et al. [13], the LSSVR is a feasible alternative for nonlinear metamodeling. In this study, the LSSVR is to be integrated with a sampling-based global optimization method, MPS.

2.1 Basic Theories of LSSVR. Consider a regression problem with a training set $\{x_i, y_i\}_{i=1}^{N}$ with N input data x_i and output data y_l as presented in Eq. (1)

$$D = \{(x_1, y_1), (x_2, y_2) \cdots (x_l, y_l) \cdots (x_N, y_N)\}, x_l \in R^n, y_l \in R \quad (1)$$

Using a kernel function, we can obtain a nonlinear predictor called LSSVR by solving an optimization problem in the primal weight space

$$\begin{aligned} &\underset{w,\varepsilon}{\text{Min}} J(w, \varepsilon) = \frac{1}{2} w^T w + \frac{1}{2} \gamma \sum_{i=1}^{N} \varepsilon_i^2 \\ &s.t. y_i = w^T \varphi(x_i) + b + \varepsilon_i, i = 1, 2, \ldots, N \end{aligned} \quad (2)$$

where $\varphi(\cdot) = R^n \Rightarrow R^{n_h}$ is a nonlinear mapping which maps the input data into a high-dimensional feature space whose dimension can be infinite; this feature helps SVR solve high-dimensional problems. In Eq. (2), $w \in R^{n_h}$ denotes the weight vector in the primal space; $\varepsilon_l \in R$ is an error variable and b is the bias term. The cost function J consists of a sum-squared error fitting error and regulation term. The γ is a constant coefficient to determine the relative importance of the empirical risk minimization and the structure risk minimization terms. It can be assigned directly. A linear SVR has been taken with $\gamma = 1$. In the case of noisy data, one avoids over fitting by taking a smaller value of γ. But, if the γ is smaller, the robustness of approximation cannot be guaranteed. Therefore, it is recommended that the value of γ can be determined by considering the kernel function coefficient together. It will be discussed later.

The model of the primal space can be presented as follows

$$y(x) = w^T \varphi(x) + b \quad (3)$$

Then, the Lagrangian multiplier expression applied to Eq. (2) is obtained as

$$L(w, b, \varepsilon, a) = J(w, \varepsilon) - \sum_{i=1}^{N} a_i \{w^T \varphi(x_i) + b + \varepsilon_i - y_i\} \quad (4)$$

Where a_i are the Lagrangian multipliers, which can be either positive or negative.

The conditions for optimality are

$$\begin{cases} \dfrac{\partial(L(w,b,\varepsilon,a))}{\partial w} = 0 \Rightarrow w = \sum_{i=1}^{N} a_i \varphi(x_i) \\ \dfrac{\partial(L(w,b,\varepsilon,a))}{\partial b} = 0 \Rightarrow \sum_{i=1}^{N} a_i = 0 \\ \dfrac{\partial(L(w,b,\varepsilon,a))}{\partial \varepsilon} = 0 \Rightarrow a_i = \gamma \varepsilon_i \\ \dfrac{\partial(L(w,b,\varepsilon,a))}{\partial a} = 0 \Rightarrow w^T \varphi(x_i) + b + \varepsilon_i - y_i = 0 \end{cases} \tag{5}$$

After elimination of w and ε, we can obtain the following linear expression

$$\begin{bmatrix} 0 & I^T \\ I & \Gamma + \frac{1}{\gamma} I \end{bmatrix} \begin{bmatrix} b \\ a \end{bmatrix} = \begin{bmatrix} 0 \\ y \end{bmatrix} \tag{6}$$

where

$$\begin{cases} y = [y_1, y_2, \ldots, y_N]^T \\ I = [1, 1, \ldots, 1]^T \\ a = [a_1, a_2, \ldots, a_N]^T \\ \Gamma_{i,j} = \varphi(x_i)^T \varphi(x_j) \, for \, i, j = 1, 2, \ldots, N \end{cases} \tag{7}$$

Based on Mercer's condition [27], there exists a mapping $\varphi(\cdot)$ and an expression

$$K(x,y) = \sum_i \varphi_i(x)^T \varphi_i(y) \tag{8}$$

If and only if, for any $\psi(x)$ such that $\int \psi(x)^2 dx$ is finite, one has

$$\int K(x,y)\psi(x)\psi(y)dxdy \geq 0 \tag{9}$$

which is motivated by Mercer's Theorem [27]. Note that for specific cases, it may not be easy to check whether Mercer's condition [27] is satisfied. Equation (9) must hold for every $\psi(x)$ with a finite L_2 norm. It is known, however, that the condition is satisfied for positive integral powers of the dot product $K(x_i, x_j)$

$$K(x_i, x_j) = \varphi(x_i)^T \varphi(x_j), \text{for } i, j = 1, 2, \ldots, N \tag{10}$$

The resulting LSSVR model for the function estimation is then obtained as

$$y(x) = \sum_{i=1}^{N} a_i K(x, x_i) + b \tag{11}$$

where a_l and b are the solutions to Eq. (5), and

$$K(x_i, x_j) = \exp\left(-(x_i - x_j)^2 \Big/ r^2\right) \tag{12}$$

Among all kernel functions, Gaussian kernel function as shown in Eq. (12) is the most popular choice and also chosen in this study. The radius r of the Gaussian kernel function is manually set in this study after a few trials for each function; x_i and x_j are input vectors. Automatically optimizing kernel function during training could potentially improve the modeling results further. The optimal choice for the kernel function is still an area of active research and will be investigated in future work. In this study, we substitute different combinations of (γ, r) into Eq. (2) and select the optimal one according to the results. In order to improve the efficiency, this procedure is implemented by the ANN method.

2.2 LSSVR-Based MPS. In this section, we propose a LSSVR-based MPS approach. MPS is an optimization algorithm which integrates metamodeling and a novel discriminative sampling strategy. For the original MPS [25,26], RBF is applied to the establishment of a sampling guidance function, but RBF is not able to filter the noisy sample points. This motivates the development of the LSSVR-based MPS. In the proposed method, LSSVR is used for replacing the linear RBF in the original MPS to construct the guidance sampling function and determine the sampling direction. New steps are also added to the original MPS procedure to check and improve the accuracy of the metamodel.

The discriminative sampling method in the original MPS is composed of the following key steps [25,26]:

1. Given an n-dimensional probability density function (PDF) $g(x)$ with compact support $S(g) \subset R^n$, a discrete space $S_N(g)$ is generated consisting of N uniformly distributed based samples in $S(g)$. N is usually larger if the dimension of $g(x)$ is higher. These uniform samples can be generated by using either the deterministic or stochastic procedures.
2. The sample points $S_N(g)$ are clustered into K contours $\{E_1, E_2, \ldots, E_K\}$ with equal size according to the relative value of the function $g(x)$. A discrete distribution $\{P_1, P_2, \ldots, P_K\}$ of the average $g(x)$ value over the K contours is built.
3. Finally, a sample is drawn from the set of all samples $S_N(g)$ according to the discrete probability distribution $\{P_1, P_2, \ldots, P_K\}$.

As a result, the generated sample points will have an asymptotic distribution as $g(x)$. For optimization, MPS treats the inverse of an objective function as $g(x)$ so that the generated sample points concentrate near the current minimum of the objective function (or maximum of $g(x)$, and yet still statistically covering the entire design space. Building on the discriminative sampling strategy, MPS integrates metamodeling and local approximation for optimization. In this study, we modified the original MPS algorithm to accommodate the LSSVR. For an n-dimensional underlying function $f(x)$ over a compact set $S(f) \subset R^n$, which is to be minimized, the modified MPS is presented as follows:

Step 1. Generate m initial sample points $x^1, x^2, \ldots, x^m$ which are uniformly distributed on $S(f)$;

Step 2. Use m function values (responses) $f(x^1), f(x^2), \cdots, f(x^m)$ to fit a LSSVR function

$$\hat{f}(x) = \sum_{i=1}^{m} a_i K(x, x_i) + b, \hat{f}(x^i) = f(x^i), i = 1, 2, \ldots, m \tag{13}$$

Step 3. Define $g(x) = c_0 - \hat{f}(x)$, where c_0 is any constant such that $c_0 \geq \hat{f}(x)$, for all x in $S(f)$. Since $g(x)$ is non-negative on $S(f)$, it can be regarded as a PDF, or a sampling guidance function, whose modes are located at x^i's, where the function values are the lowest among $\{\hat{f}(x^i)\}$. Then the above sampling algorithm is used for generating a random sample from $S(f)$ according to $g(x)$. These sample points have the tendency to concentrate about the maximum of $g(x)$, which corresponds to the minimum of $\hat{f}(x)$.

Step 4. Combine the sample points generated at step 3 with the initial samples in step 1 to form the new set $x^1, x^2, \ldots, x^{2m}$.

Step 5. In this step, leave-one-out cross-validation (LOOCV) is used for obtaining R^2 for each sample point.

$$R^2_{avg} = \frac{\sum_{i=1}^{m} \left(1 - \sum_{i=1}^{m-1} \frac{(y_i - \hat{y}_i)^2}{(y_i - \bar{y}_i)^2}\right)}{n} \tag{14}$$

For mathematical problems, the convergence condition should be set strictly, such as $R^2_{avg} > 0.8$. For the engineering problems, the convergence condition can be slacked according to the complexity of the case. This step is applied only to the expensive sample points whose responses are obtained from the computational intensive simulations. If the convergence condition is met, the procedure ends, otherwise goes to step 6.

Step 6. Find the sample point possessing the minimal R^2 value and a neighboring sample point that has the next smallest R^2 value. A new sample point is generated in between the two points and then evaluated by calling the expensive simulation. Then this point is added to the point set defined in step 4 and goes back to Step 2.

In addition to the use of LSSVR to replace RBF at step 2, Steps 5 and 6 are new additions to the original MPS to enrich the sample set at where the modeling error is large in order to improve the accuracy of the metamodel. This is similar to the approach used in the EGO where the new sample points are generated in areas of the potential accuracy improvement.

3 Benchmarking of the Proposed Method

The performance of the proposed approach can be evaluated from the following aspects: accuracy and robustness of the metamodel, accuracy of optimum results, and efficiency of the optimization procedure.

3.1 Test Functions. Mathematical test functions are selected from the book of Hock and Schittkowski [28], which offers 180 problems for testing the nonlinear optimization algorithms. Jin et al. [29] used 13 from these180 functions to test the performance of different types of metamodels. From the application of these test problems in literature [25,29], we selected 11 nonlinear problems, which are listed in Table 1. Most of these problems are known to be of highly nonlinear such as Rastrigin, Rosenbrock, Schwefel, and Griewank problems, and/or be multimodal in nature, such as Griewank, Dixon and Price, and Hartman problems. These selected problems are often used to benchmark either metamodels or global optimization algorithms. Moreover, according to Ref [25], the MPS has been proved efficient for low dimensional problems. Therefore, more high-dimensional functions are selected in this work for testing, which are defined as follows in Table 1. According to Step 5 in Sec. 2.2, we need to define the criterion in Eq. (4). For these cases, R^2_{avg} is set to be 0.9.

3.2 Performance Metrics. To evaluate the performance of LSSVR, a systematic comparison is conducted to analyze its strengths and weaknesses with four popular metamodeling techniques: ANN, RBF, KG, and MARS. Three error metrics and their derivations are used for evaluating the metamodeling performance on both the accuracy and robustness. All metamodels are based on the final updated samples generated by the modified MPS method. The efficiency and accuracy of the LSSVR-based MPS optimization method are considered in Sec. 3.2.3.

In this study, LOOCV is applied to obtaining the performance metrics for the metamodeling techniques. Cross-validation is a statistical practice of partitioning a sample of data into subsets such that the analysis is performed on one subset, while the other subset(s) are retained for subsequent use in validating the initial analysis. LOOCV uses a single observation from the original sample as the validation data and the remaining observations as the training data. This is repeated such that each observation in the sample set is used once as the validation data.

3.2.1 Accuracy of Metamodel. The accuracy is an important indicator of a metamodel's performance. The accuracy metrics should reflect the metamodel output $\hat{y}_i$'s deviation from the simulation output y. LOOCV introduced by Mitchell and Morris [30] is used for assessing the accuracy of the proposed approach. The mean squared error (MSE), average absolute error (AAE), and mean absolute error (MAE) are applied to estimating the accuracy of the current metamodel. The expressions for these three criteria are given in the following equations, respectively

$$\mathrm{MSE} = \frac{1}{N}\sum_{i=1}^{N}\left(y_i - \hat{y}_i\right)^2 \tag{15}$$

where $\hat{y}_i$ is the corresponding predicted value for the observed value y_i. The MSE represents the departure of the metamodel from the simulation model

$$\mathrm{AAE} = \frac{\sum_{i=1}^{N}\left|y_i - \hat{y}_i\right|}{N} \tag{16}$$

$$\mathrm{MAE} = \mathrm{MAX}\left(\left|y_i - \hat{y}_i\right|\right) \tag{17}$$

Generally smaller values of AAE and MAE indicate more accurate metamodels.

To stay objective, MSE, AAE, and MAE are calculated from the test sample points, not on the modeling points. Therefore, $\hat{y}_i$ is the predicted function value at the test sample points.

As described in Sec. 3.1, the mathematical problems have different output ranges. In order to obtain a more comparative measure of accuracy across different problems, a new type of accuracy metrics proposed by Clarke et al. [13] is used in the study. Instead of the direct metrics in Eqs. (15), (16), and (17), a relative error criterion is used for benchmarking. The expression of the relative error can be written as

$$\mathrm{RERR} = \frac{\mathrm{ERR}(\bullet) - \mathrm{ERR}(\mathrm{LSSVR})}{\mathrm{ERR}(\mathrm{LSSVR})} \tag{18}$$

where $(\bullet)$ denotes other metamodeling techniques. The ERR (error) in Eq. (18) refers to the errors defined in Eqs. (15–17). As LSSVR is the metamodeling technique under study, we use it as the benchmark. For each test problem, RERR (relative ERR) is obtained for each metamodel method such that a positive value indicates that the method in comparison has a larger error than the LSSVR, while a negative value indicates that the method in comparison obtains a smaller error than the LSSVR. RERR for LSSVR equals to zero.

3.2.2 Robustness of Metamodel. Robustness is another important indicator of performance as it represents each method's ability to consistently achieve similar accuracies on different problems. According to the suggestion of Jin et al. [27], the robustness is defined as the standard deviation of one method's error values across different problems. Similar to the accuracy measure, we use LSSVR as the benchmark to calculate the standard deviation of the relative errors for other types of metamodels. The formula of the relative robustness is given as

$$\mathrm{STD\ RERR} = \mathrm{STD}(\mathrm{RERR}) \tag{19}$$

where RERR is expressed in Eq. (18) and STD stands for the standard deviation. STD (RERR) for the LSSVR equals to zero.

3.2.3 Accuracy and Efficiency of Optimization. To validate the proposed optimization method, the accuracy of the optimum results and efficiency of the optimization procedure are also considered. The proposed LSSVR-based MPS optimization method is tested using the test problems listed in Table 1, in comparison with several well-known metamodel-based optimization methods, such as PSOIS [23], successive response surface approximations (SRSM) [31], and MPS algorithm [25,26]. To compare the accuracy and efficiency of these optimization methods, the number of evaluations (NOE) is used to assess the efficiency of the proposed method. Additionally, to compare all algorithms objectively,

Table 1 Description of test functions

Function name	Dimension (N)	Expression	Interval	Global min.
Colville	4	$f(x) = 100(x_1^2 - x_2)^2 - (x_1 - 1)^2 + (x_3-)^2 + 90(x_3^2 - x_4)^2 + 10.1((x_2 - 1)^2 + (x_4 - 1)^2) + 19.8(x_2 - 1)(x_4 - 1)$	$x_i \in [-10, 10]$	0
De Jong	10	$f(x) = \sum_{i=1}^{N} x_i^2$	$x_i \in [-5.12, 5.12]$	0
Dixon and Price	10	$f(x) = (x_1 - 1)^2 + \sum_{i=2}^{N} i(2x_i^2 - x_{i-1})^2$	$x_i \in [-10, 10]$	0
Rastrigin	10	$f(x) = 10N + \sum_{i=1}^{N} [x_i^2 - 10\cos(2\pi x_i)]$	$x_i \in [-5.12, 5.12]$	0
Schwefel	10	$f(x) = \sum_{i=1}^{N} [-x_i \sin(\sqrt{\lvert x_i \rvert})]$	$x_i \in [-500, 500]$	418.9829 N
Rosenbrock	10	$f(x) = \sum_{i=1}^{N} \left(100(x_{i+1} - x_i^2)^2 + (x_i - 1)^2\right)$	$x_i \in [-2.048, 2.048]$	0
Griewank	10	$f(x) = \frac{1}{4000}\sum_{i=1}^{N}(x_{i+1} - 100)^2 - \prod_{i=1}^{n}\cos\left(\frac{(x_i - 100)}{\sqrt{i}}\right) + 1$	$x_i \in [-300, 300]$	1
Hartman	6	$f(x) = -\sum_{i=1}^{4} c_i \exp\left[-\sum_{j=1}^{N} a_{ij}(x_j - p_{ij})^2\right]$ $[a_{ij}]_{j=1,\ldots 6} = \begin{bmatrix} 10 & 3 & 17 & 3.5 & 1.7 & 8 \\ 0.05 & 10 & 17 & 0.1 & 8 & 14 \\ 3 & 3.5 & 1.7 & 10 & 17 & 8 \\ 17 & 8 & 0.05 & 10 & 0.1 & 14 \end{bmatrix}$ $c_i = [1 \quad 1.2 \quad 3 \quad 3.2]$ $[p_{ij}]_{j=1,\ldots 6} = \begin{bmatrix} 0.1312 & 0.1696 & 0.5569 & 0.0124 & 0.8283 & 0.5886 \\ 0.2329 & 0.4139 & 0.8307 & 0.3736 & 0.1004 & 0.9991 \\ 0.2348 & 0.1451 & 0.3522 & 0.2883 & 0.3047 & 0.6650 \\ 0.4047 & 0.8828 & 0.8732 & 0.5743 & 0.1091 & 0.0381 \end{bmatrix}$	$x_i \in [0, 1]$	−3.32237
Ackley	10	$f(x) = -ae^{-b\left(\sqrt{\sum_{i=1}^{n} x_i^2 \Big/ N}\right)} - e^{\sum_{i=1}^{n}\cos(cx_i) \Big/ N} + a + e$ $a = 20, b = 0.2, c = 2\pi$	$x_i = [-32.768, 32.768]$	0
Levy	10	$f(x) = \sin^2(\pi y_1) + \sum_{i=1}^{N}\left((y_i - 1)^2(1 + \sin^2(\pi y_1 + 1)\right) + (y_n - 1)^2(1 + 10\sin^2(2\pi y_n)), y_i = 1 + \frac{x_i - 1}{4}$	$x_i \in [-10, 10]$	0
A function of 16 variables (F16)	16	$f(x) = \sum_{i=1}^{16}\sum_{j=1}^{16} a_{ij}(x_i^2 + x_i + 1)(x_j^2 + x_j + 1)$ $x_i, x_j \in [-1, 1], i, j = 1, 2, \ldots 16$	$x_i \in [-1, 1]$	25.887

ARERR (average relative error) described in Eq. (20) is used as the convergence condition for all the methods.

$$\text{ARRE} = \frac{\sum_{i=1}^{n}\left|\frac{\text{AOPTI}^i - \text{OPTI}^i}{\text{AOPTI}^i}\right|}{n} \tag{20}$$

where n denotes the number of design variables, AOPTI and OPTI mean the analytical and obtained optimum values, respectively. If ARRE > 0.9, the optimization procedure stops.

3.3 Test Procedure and Results. To assess the accuracy of the results, MSE, AAE, and MAE are calculated in the relative expression as defined in Eq. (18). The resulting related errors for ANN, RBF, KG, and MARS are listed in Fig. 1(*a*). Figure 1(*a*) shows the percentages by which the average error values are higher than the corresponding error values for the LSSVR, if the values are positive. Conversely if the values are negative, it means the model has a smaller error than the LSSVR. These percentage differences have been averaged over all given test functions. Overall as no negative values in the figure, it means that the LSSVR has outperformed the other four approximation techniques with smaller errors. Among the rest of approaches, KG demonstrates good accuracy globally (low MSE values) and on local regions (low AAE and MAE values).

To further compare the robustness of each algorithm, Fig. 1(*b*) presents the normalized standard deviations of the errors for each approximation technique, relative to LSSVR. The results indicate that the LSSVR is the most robust of the five approximation

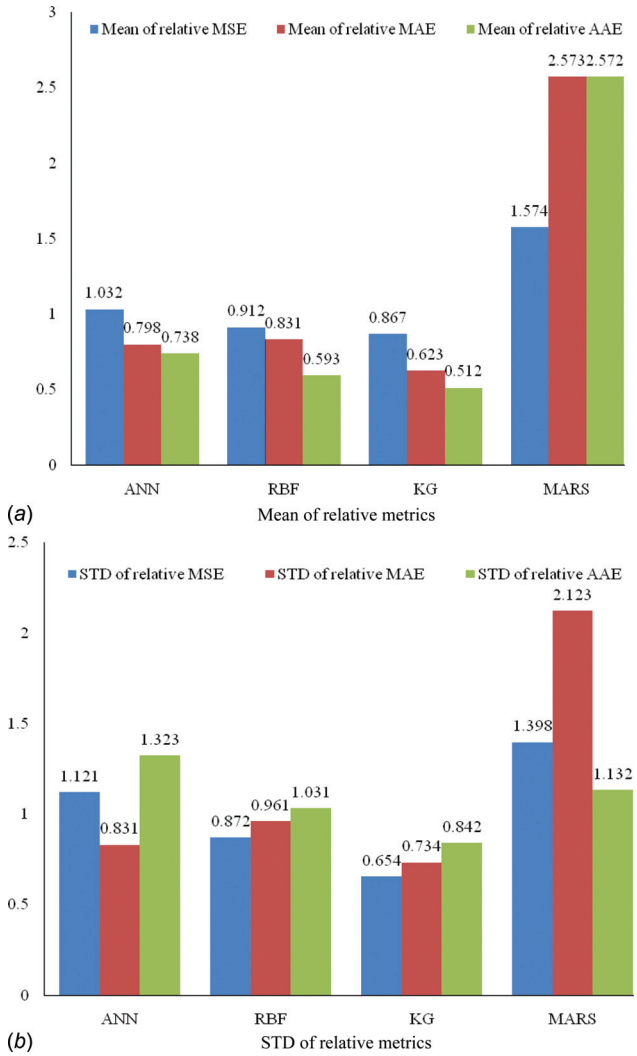

Fig. 1 Relative performance of metamodeling approaches with respect to LSSVR. (*a*) Mean of relative metrics; (*b*) STD of relative metrics.

methods. KG and RBF are the second and third most robust metamodeling methods. MARS and ANN have very large variances, which implies that the MARS and ANN may not be suitable for high-dimensional nonlinear function approximation.

Figure 2 demonstrates the efficiency comparisons between the proposed LSSVR-based MPS with the other metamodel-based approaches including PSOIS, SRMS, and the original MPS; one can see that the proposed method is noticeably more efficient. The LSSVR-MPS is also compared with the global optimization methods, such as genetic algorithm (GA), simulated annealing (SA), and particle swarm optimization (PSO). The efficiency of the LSSVR-based MPS, as well as the other metamodel-based methods, is in general significantly higher than those heuristics methods.

To summarize the test results, we find that the LSSVR is overall more efficient and robust than other approaches for the chosen set of nonlinear test problems with relatively high dimensionality. The integrated LSSVR-MPS optimization approach demonstrates higher efficiency than the other chosen optimization approaches. Section 4 will discuss the application of the proposed approach to three different crashworthiness design problems.

4 Crashworthiness Optimization

In this section, the proposed LSSVR-based MPS is applied to three typical crashworthiness problems. The first example studies a fontal member of a vehicle under impact; it is relatively simple, small in scale, but representative of features of a crashworthiness problem. The preliminary study for the proposed method is based on this case. In order to compare the performance of metamodeling-based optimization methods, the original MPS, PSOIS, and SRSM are also applied to optimizing this case. All new car models by law must pass certain safety tests with frontal and side compacts before they are sold. Therefore the second and third cases consider full vehicle collisions at the front and side, respectively. These two cases are comparatively more complicated than the first case. As discussed before, the crash simulation procedure involves noises and even outliers from the numerical computation. The high computational costs and high nonlinearity of the crashworthiness problem prohibit us from creating a trustworthy uncertainty model. In this work, we applied two measures to identifying the simulation outputs with excessive errors. First, total impact energy for crash simulation, which is the sum of internal (potential) and external (kinetic) energy, should remain constant, assuming the heat loss is negligible. In practice, the total energy might not be in balance due to the use of some numerical methods, such as hourglass control. When the sum of internal and external energy is

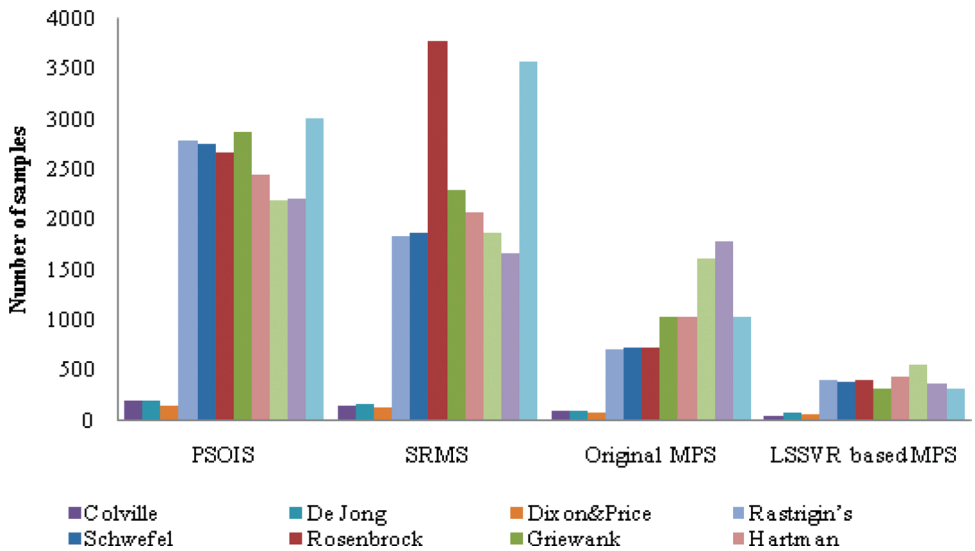

Fig. 2 Efficiency comparison of optimization approaches

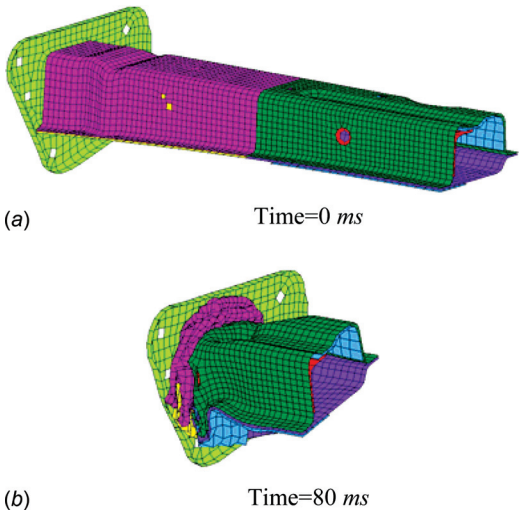

Fig. 3 FE model of the vehicle frontal member under impact

larger than 95% of the total energy, the simulation result is regarded as acceptable. Otherwise, we deem the error is excessive and the obtained design point is discarded. Second, in this study we use LS-DYNA as the simulation toolkit and the one point integration shell element proposed by Belytschko and Tsay (B.T. element) [32] for crash simulation. In order to guarantee the accuracy and stability of the B.T. element for buckling, the number of warp elements is calculated. If this value is larger than 10% of the total number of all shell elements, the corresponding sample point is considered as an outlier and thus discarded. After two checks, the noises in the data are deemed random and could be handled by the LSSVR. Moreover, as we mentioned before, since the crashworthiness optimization is a high nonlinear problem, the criterion R^2_{avg} described in step 5 in Sec. 2.2 is relaxed to 0.7.

4.1 Case I: Impact on a Vehicle Frontal Member

4.1.1 Problem Description. The FE model of a frontal member of a vehicle is presented in Fig. 3. It is composed of 11 parts. It is modeled with 5359 nodes and 4946 elements (the number of shell elements is 4900). The structure is fixed at the rear end and a rigid wall impacts the front. The frontal number has an initial velocity of 14 m/s and a mass of 1.21 kg. The model takes about 10 min for each FEA evaluation on a Dell Precision T3400 (Intel™ Core®2 Duo, 3.0 GHz/1333 MHz/4 MB) workstation.[1]

The objective function is to minimize the maximum rigid wall force. Eight thicknesses of individual parts of the frontal member are selected as design variables. The bounds and initial values of design variables are listed in Table 2. Although the thickness design variable (unit, mm) is continuous, to save the computational cost and make design variables more usable, only three effective digits are kept. For example, 1.599999 should be regarded as 1.60. This strategy is also applied to cases II and III.

Table 2 Design variables and bounds for case I

Design variables (mm)	Part ID	Initial value	Intervals
x_1	804	1.80	[1.0, 3.0]
x_2	806	1.80	[1.0, 3.0]
x_3	80256	1.50	[1.0, 3.0]
x_4	82046	2.20	[1.0, 3.0]
x_5	82047	2.20	[1.0, 3.0]
x_6	82049	2.50	[1.0, 3.0]
x_7	82068	3.00	[2.0, 4.0]
x_8	82095	2.50	[1.0, 3.0]

The optimization problem is described as

$$\text{Min}(\text{Max}(F_{rw}(X))) \tag{21}$$

subject to

$$\frac{F_{\text{mass}}(X_{\text{initial}})}{F_{\text{mass}}(X_{\text{opt}})} > 1 \tag{22}$$

$$\frac{F_{\text{ieng}}(X_{\text{initial}})}{F_{\text{ieng}}(X_{\text{opt}})} < 1 \tag{23}$$

Where $F_{rw}(X)$ and $F_{\text{ieng}}(X)$ are the peak rigid wall force and energy function, respectively; X_{initial} and X_{opt} denote the initial and optimum design variables, respectively.

4.1.2 Optimization Procedure and Results. As mentioned before, the LSSVR-based MPS, the original MPS, PSOIS, and SRSM are applied to this problem. To control the computation cost, the number of sample points (NOS) for each method is limited to 200. In addition, to avoid unrepresentative results, five different runs are carried out for each optimization method. The average and best optimum results are presented in Table 3. The change in the rigid wall force with respect to time for the initial and optimum design variables by different methods are presented in Fig. 4. According to Table 3 and Fig. 4, it is easy to observe that the LSSVR-based MPS achieves the best optimum solution and corresponding average optimum result is also good. Compared with the NOS of other methods, the proposed method is the most efficient. Therefore, we use more complicated crashworthiness optimization problems, cases II and III, to verify the performance of the proposed strategy in Section 4.2.

4.2 Case II: Full Vehicle Frontal Collision

4.2.1 Problem Description. Our crashworthiness metamodeling problem is based on a reduced full-scale FE model of a minicar. It consists of 20 types of materials and 207 parts. It is modeled with 19,226 nodes and 16,132 elements (the number of shell elements is 15,300). This model is used for the frontal impact simulation and has been validated with physical crash test data. The original FE model 100 ms before and after a frontal impact at 55.69 km/h is shown in Fig. 5. The model takes about 1 h for each FEA evaluation. The objective function of crashworthiness design

Table 3 Optimum results of case I

Method	Design variables (*mm*)								F_{rw} (KN)	NOS
MPS (Best)	1.39	2.00	2.06	1.09	1.07	1.35	3.83	1.48	145.12	139
MPS (Average)	1.07	1.77	1.01	1.39	1.12	1.25	3.41	1.13	150.34	200
LSSVR-based MPS (Best)	1.05	2.62	1.13	1.00	1.03	2.83	3.26	1.13	121.23	123
LSSVR-based MPS (Average)	1.04	2.52	1.21	1.02	1.04	2.73	3.12	1.17	127.32	138
PSOIS (Best)	1.89	1.13	1.25	1.04	1.48	1.25	3.60	1.10	128.86	185
PSOIS (Average)	1.51	1.23	1.52	1.03	1.27	1.65	3.34	1.18	153.86	179
SRSM (Best)	1.07	2.41	1.07	1.07	1.05	1.72	2.41	1.31	163.14	200
SRSM (Average)	1.09	2.43	1.05	1.09	1.73	2.24	2.96	1.99	168.74	200

[1]FE simulations in this study are performed on this workstation.

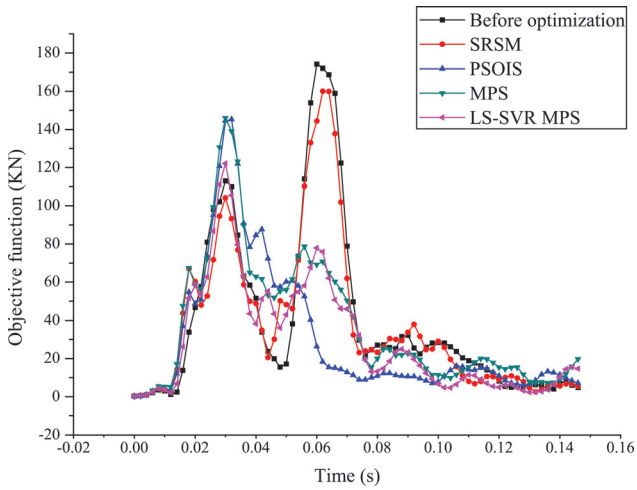

Fig. 4 Change in the rigid wall force with respect to time for the initial and optimum design variables of case I

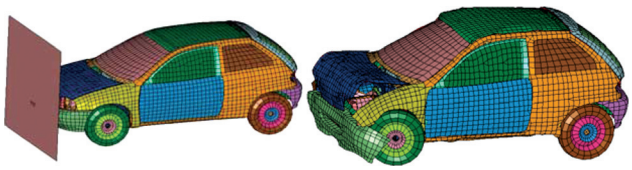

Fig. 5 Crash simulation result with optimum design variables for case II

in this case is to maximize the energy absorption capacity of the vehicle. There are 13 design parameters used in the optimization. The bounds of the design variables are listed in Table 4.

The optimization problem is given by

$$\mathrm{Max}\left(F_{\mathrm{ieng}}(X)\right) \tag{24}$$

subject to

$$\frac{F_{\mathrm{mass}}(X_{\mathrm{initial}})}{F_{\mathrm{mass}}(X_{\mathrm{opt}})} > 1 \tag{25}$$

$$\frac{F_{\mathrm{acc}}(X_{\mathrm{initial}})}{F_{\mathrm{acc}}(X_{\mathrm{opt}})} > 1 \tag{26}$$

Where $F_{\mathrm{ieng}}(X)$ is the internal energy, $F_{\mathrm{ass}}(X_{\mathrm{initial}})$ and $F_{\mathrm{ass}}(X_{\mathrm{opt}})$ denote the acceleration with the initial and optimum design variables, respectively.

Table 4 Design variables and bounds of case II

Design variables	Part ID	Initial value	Intervals	Optimum value
x_1	48	1.0	[0.8, 1.5]	0.92
x_2	50	0.8	[0.6, 1.2]	0.75
x_3	51	2.2	[2.0, 2.8]	2.51
x_4	52	2.2	[2.0, 2.8]	2.03
x_5	58	2.3	[1.8, 2.7]	2.05
x_6	59	2.3	[2.0, 2.5]	2.16
x_7	60	1.0	[0.6, 1.5]	0.87
x_8	61	1.0	[0.6, 1.5]	0.76
x_9	102	1.5	[1.0, 2.0]	0.78
x_{10}	122	0.7	[0.5, 1.2]	0.90
x_{11}	123	0.7	[0.5, 1.2]	0.82
x_{12}	135	0.7	[0.5, 1.2]	0.63
x_{13}	136	0.7	[0.5,1.2]	0.72

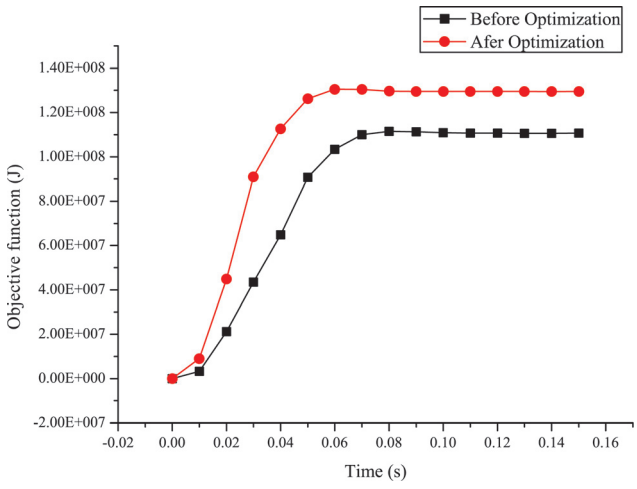

Fig. 6 Change of internal energy of initial and optimum designs of case II

4.2.2 Optimization Procedure and Results. For this case, the NOS is limited to 300. To reduce the NOS, we also keep three effective digits for all values of design variables as in Case I. Due to the scale of this case, only the LSSVR-based MPS is performed. After 197 iterations, the optimum result is achieved as shown in Table 4 and the corresponding crash status is presented in Fig. 5. The change in the internal energy of initial and optimum design is shown in Fig. 6.The optimum design effectively improves the energy absorption capacity of the vehicle.

4.3 Case I: Full Vehicle Side Collision

4.3.1 Problem Description. The side impact simulation in this case is performed with a movable barrier impacting the vehicle perpendicularly at a speed of 50 km/h. The computer environment is the same as in Cases I and II. In order to improve the simulation accuracy, a detailed full scale FE model of the vehicle has been established, including body assembly, engine, drive system, and tires. The FE model, containing 98,249 shell elements, 4562 solid elements, 7213 beam elements, and 4124 mass elements, consists of 298 parts, which is shown in Fig. 7. The model takes about 2.5 h for each FEA evaluation.

The design objective is to minimize the deflection at test point 1 presented in Fig. 8 during impact

$$\mathrm{Max}\left(F^{1}_{\mathrm{def}}(X)\right) \tag{27}$$

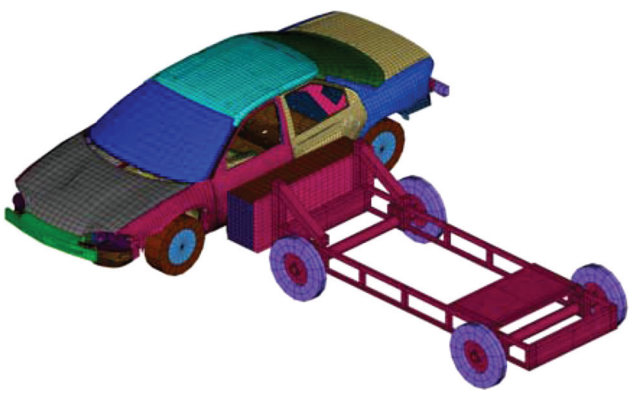

Fig. 7 FE model of side impact for case III

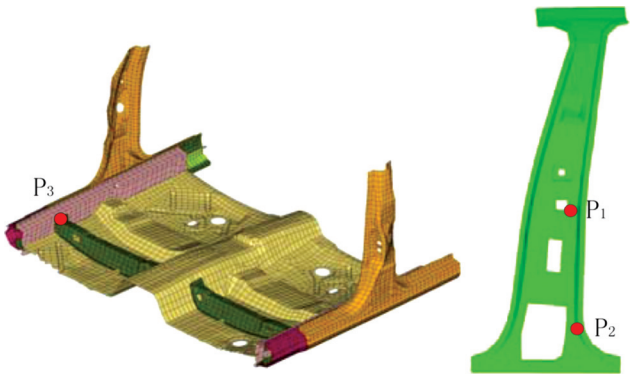

Fig. 8 Location of test points (P_1 are P_2 locate on the B-pillar; P_3 locates on the floor)

subject to

$$\begin{cases} F_{\text{vel}}^1 < 8.5 \text{ m/s} \\ F_{\text{vel}}^2 < 8.5 \text{ m/s} \\ F_{\text{vel}}^3 < 6 \text{ m/s} \\ F_{\text{def}}^2 < 0.3 \text{ m} \\ F_{\text{def}}^3 < 0.2 \text{ m} \end{cases} \tag{28}$$

Where F_{vel}^i and F_{def}^i denote the maximum velocity and reflection at test point i, respectively. They are measured at the middle and bottom of the B-pillar (P_1 and P_2) and the floor (P_3) as presented in Fig. 8.

There are ten thicknesses of the selected components as design parameters used in the design optimization of vehicle side impact as shown in Fig. 9, the deflection curve before and after optimization is demonstrated in Fig. 10 and the optimum results are listed in Table 5. It demonstrates that the maximum deflection in P_1 has been reduced successfully.

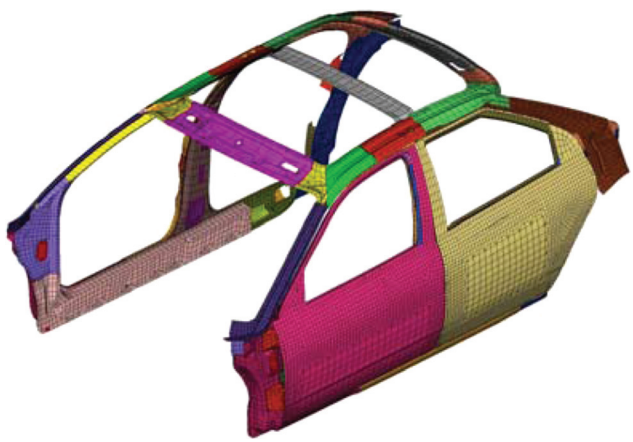

Fig. 9 Selected components that need optimization

Table 5 Design variables and bounds of case III

Design variables	Part ID	Initial value	Intervals	Optimum value
x_1	123	1.0	[0.5, 1.5]	0.83
x_2	124	1.0	[0.5, 1.5]	0.92
x_3	125	1.0	[0.5, 1.5]	1.02
x_4	126	1.0	[0.5, 1.5]	1.32
x_5	127	1.0	[0.5, 1.5]	0.97
x_6	128	1.0	[0.5, 1.5]	1.23
x_7	129	2.0	[1.0, 3.0]	1.76
x_8	130	1.5	[1.0, 3.0]	2.08
x_9	131	1.0	[0.5, 1.5]	0.91
x_{10}	132	1.0	[0.5, 1.5]	0.82

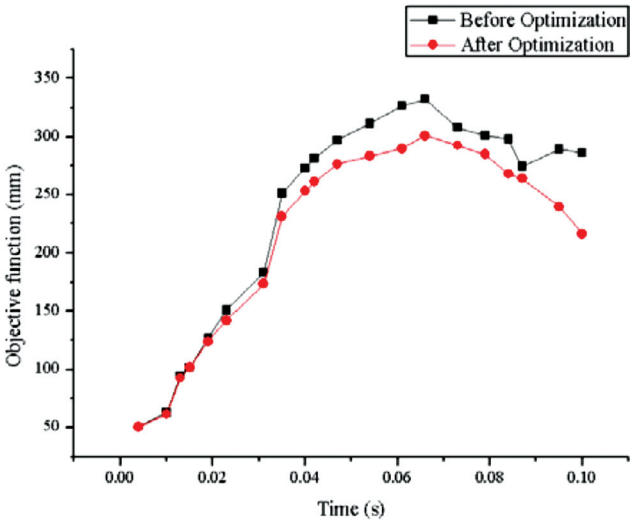

Fig. 10 Change of deflection of B pillar with initial and optimum designs of case III

5 Conclusions

In this paper, a metamodeling-based optimization technique is proposed. An intelligent sampling strategy, MPS, is used for generating the sample points in optimization procedure. The advantage of the MPS is that newly generated samples concentrate near the current local minima and yet still statistically cover the entire design space. Therefore, the corresponding metamodel is constructed based on more attractive sample points for the purpose of optimization. The original MPS uses RBF to establish the sampling guidance function, but the RBF is not robust in filtering the noisy points. Therefore, the recently developed LSSVR is employed to replace RBF, which can also help to filter noises in data. To assess the performance of the LSSVR-based MPS optimization method, the performance of metamodeling and optimization is tested. Compared with the other four popular metamodeling techniques, LSSVR is proved to be the most attractive method for integration with MPS. Furthermore, to verify the accuracy and efficiency of the proposed method, the other metamodel-based optimization methods including MPS, PSOIS, and SRSM are also tested. According to benchmark tests, the superiority of the LSSVR-based MPS is evident.

Our purpose is to develop a feasible optimization approach for crashworthiness design. Thus, we apply the LSSVR-based MPS to three different crashworthiness problems, including component, full vehicle frontal, and side impacts. These problems are successfully optimized by the proposed method. The tests demonstrate that the proposed method shows a potential for the crashworthiness problems.

Acknowledgment

Funding from Natural Science and Engineering Research Council (NSERC) of Canada, National Natural Science Foundation of China (10902037), and National Basic Research Program (973) of China (60635020) are acknowledged. The authors would also like to thank anonymous reviewers for their constructive comments, the National High Technology Research and Development Program ("863" Program) of China under Grant No. 2009AA044501; Program for Changjiang Scholars and Innovative Research Team in University and the State Key Laboratory of Advanced technology for vehicle design and manufacture are acknowledged.

References

[1] Kurtaran, H., Eskandarian, A., Marzougui, D., and Bedewi, N. E., 2002, "Crashworthiness Design Optimization Using Successive Response Surface Approximations," Comput. Mech., **29**(4–5), pp. 409–421.

[2] Gu, L., 2001, "A Comparison of Polynomial Based Regression Models in Vehicle Safety Analysis," *Proceedings of ASME Design Engineering Technical Conferences*, Pittsburgh, PA, September, Paper No. DAC-21063.

[3] Yang, R. J., Wang, N., Tho, C. H., Bobineau, J. P., and Wang, B. P., 2005, "Metamodeling Development for Vehicle Frontal Impact Simulation." ASME J. Mech. Des., **127**(5), pp. 1014–1021.

[4] Forsberg, J., and Nilsson, L., 2005 "On Polynomial Response Surfaces and Kriging for Use in Structural Optimization of Crashworthiness," Struct. Multidiscip. Optim., **29**(3), pp. 1615–1488.

[5] Forsberg. J., and Nilsson. L., 2006, "Evaluation of Response Surface Methodologies Used in Crashworthiness Optimization," Int. J. Impact Eng., **32**(5), pp. 759–777.

[6] Fang, H., Rais-Rohani, M., Liu, Z., and Horstemeyer, M. F., 2005, "A Comparative Study of Metamodeling Methods for Multiobjective Crashworthiness Optimization," Comput. Struct., **83**, pp. 2121–2136.

[7] Wang, H., Li, E., Li, G. Y., and Zhong, Z. H., 2008, "Development of Metamodeling Based Optimization System for High Nonlinear Engineering Problems," Adv. Eng. Software, **39**(8), pp. 629–645.

[8] Redhe, M. and Nilsson, L. A., 2006, "Multipoint Version of Space Mapping Optimization Applied to Vehicle Crashworthiness Design," Struct. Multidiscip. Optim., **31**(2), pp. 134–146.

[9] Yang, H., Chan, L., and King, I., 2002, "Support Vector Machine Regression for Volatile Stock Market Prediction," Lect. Notes in Comput. Sci., **2412**, pp. 391–396.

[10] Yang, H., King, I., and Chan, L., 2002, "Non-Fixed and Asymmetrical Margin Approach to Stock Market Prediction Using Support Vector Regression," *Proceedings of the International Conference on Neural Information Processing (ICONIP2002)*, Singapore.

[11] Wu, C. H., Ho, M. J., and Lee, D. T., 2003, "Travel Time Prediction With Support Vector Regression," IEEE Trans. Intell. Transp. Syst., **5**, pp. 276–81.

[12] Cherkassky, V., and Ma, Y., 2004, "Comparison of Loss Functions for Linear Regression," IEEE Trans. Neural Netw., **1**(25–29), pp. 400–405.

[13] Clarke, S. M., Griebsch, J. H., and Simpson, T. W., 2005, "Analysis of Support Vector Regression for Approximation of Complex Engineering Analyses," ASME, J. Mech. Des., **127**(6), pp. 1077–1087.

[14] Suykens, J. A. K. and Vandewalle, J., 1999, "Least Squares Support Vector Machine Classifiers," Neural Process. Lett., **9**, pp. 293–300.

[15] Box, G. E. P. and Draper, N. R., 1969, *Evolutionary Operation: A Statistical Method for Process Management*, Wiley, New York.

[16] Chen, W., Allen, J. K., Schrage, D. P., and Mistree, F., 1997, "Statistical Experimentation Methods for Achieving Affordable Concurrent Systems Design," AIAA J., **35**(5), pp. 893–900.

[17] Wujek, B. A., and Renaud, J. E., 1998, "New Adaptive Move-Limit Management Strategy for Approximate Optimization–Part 1," AIAA J., **36**(10), pp. 1911–1921.

[18] Wujek, B. A., and Renaud, J. E., 1998, "New Adaptive Move-Limit Management Strategy for Approximate Optimization–Part 2," AIAA J., **36**(10), pp, 1922–1934.

[19] Toropov, V., van Keulen, F., Markine, V., and de Doer, H., 1996, "Refinements in the Multi-Point Approximation Method to Reduce the Effects of Noisy Structural Responses," *Proceedings 6th AIAA/USAF/NASA/ISSMO Symposium on Multidisciplinary Analysis and Optimization*, Vol. **2**, AIAA, Bellevue, WA, September, Paper No DETC/DAC-1451.

[20] Alexandrov, N., Dennis, J. E. J., Lewis, R. M., and Torczon, V., 1998, "A Trust Region Framework for Managing the Use of Approximation Models in Optimization," Struct. Optim., **15**(1), pp. 16–23.

[21] Jones, D. R., Schonlau, M., and Welch, W. J., 1998, "Efficient Global Optimization of Expensive Black Box Functions," J. Global Optim., **13**, pp. 455–492.

[22] Wang, G. G., and Simpson, T. W., 2001, "Fuzzy Clustering Based Hierarchical Metamodeling for Design Space Reduction and Optimization," Eng. Optimiz., **36**(3), pp. 313–335.

[23] Wang, H., Li, G. Y., and Zhong, Z. H., 2008, "Optimization of Sheet Metal Forming Processes by Adaptive Response Surface Based on Intelligent Sampling Method," J. Mater. Process. Technol., **197**(1–3), pp. 77–88.

[24] Wang H., Li E., and Li G., 2010,"Parallel Boundary and Best Neighbor Searching Sampling Algorithm for Drawbead Design Optimization in Sheet Metal Forming," Struct Multidiscip Optim., **41**(2), pp. 309–324.

[25] Wang, L., Shan, S., and Wang, G. G., 2004, "Mode-Pursuing Sampling Method for Global Optimization on Expensive Black-Box Functions," Eng. Optimiz., **36**(4), pp. 419–438.

[26] Sharif, B., Wang, G. G., and Mekkawy, T., 2008, "Mode Pursing Sampling Method for Variable Optimization on Expensive Black-Box Functions," ASME J. Mech. Des., **130**, p. 021402.

[27] Mercer. J., 1969, "Functions of Positive and Negative Type and Their Connection With the Theory of Integral Equations," Philos. Trans. R.. Soc. London, **83**(559), pp. 69–70.

[28] Hock, W. and Schittkowski, K., 1981, *Test Examples for Nonlinear Programming Codes*, Springer, New York.

[29] Jin, R., Chen, W., and Simpson, T. W., 2001, "Comparative Studies of Metamodelling Techniques Under Multiple Modelling Criteria," Struct. Multidiscip. Optim., **23**, pp. 1–13.

[30] Mitchell, T. J., and Morris, M. D., 1992, "Bayesian Design and Analysis of Computer Experiments: Two Examples," Stat. Sin. **2**, pp. 359–379.

[31] Kurtaran, H., Eskandarian, A., Marzougui D., and Bedewi, N. E., 2002, "Crashworthiness Design Optimization Using Successive Response Surface Approximations," Comput. Mech., **29**, pp. 409–421.

[32] Belytschko, T., Lin, J. I., and Tsay, C. S., 1984. "Explicit Algorithms for the Nonlinear Dynamics of Shells," Comput. Methods Appl. Mech. Eng., **42**, pp. 225–251.